
Chapter C-IV-6

Time-reversal Waveform Preconditioning for Clutter Rejection

Trond Varslot¹, Birsen Yazıcı², Evren Yarman³, Margaret Cheney⁴, Louis Scharf⁵

¹*Department of Applied Mathematics
Australian National University
Canberra, Australia
Email: trond@varslot.net*

²*Department of Electronics Computers and Systems Engineering
Rensselaer Polytechnic Institute
Troy, NY 12180
Email: yazici@ecse.rpi.edu*

³*Department of Electronics Computers and Systems Engineering
Rensselaer Polytechnic Institute
Troy, NY 12180
Email: yarman@ecse.rpi.edu*

⁴*Department of Mathematical Sciences
Rensselaer Polytechnic Institute
Troy, NY 12180
Email: cheney@rpi.edu*

⁵*Department of Engineering
Colorado State University
Fort Collins, CO 12180
Email: scharf@engr.colostate.edu*

Abstract

A time-reversal implementation of a transmit waveform *preconditioning* scheme for optimal clutter rejection in radar imaging is presented. Waveform preconditioning involves determining a map on the space of transmit waveforms, and then applying this map to the waveforms before transmission. Our work applies to antenna arrays with an arbitrary number of transmit- and receive elements, and makes no assumptions about the elements being co-located. By our time-reversal implementation we avoid the need to obtain an explicit model for the environment in order to compute the preconditioning operator.

1. Introduction

In radar applications, the scene (everything in the radar beam) is composed of three classes: objects of interest, objects which are not of interest, and (known) background. Objects of interest are referred to as *targets*, while those objects which are not of interest are referred to as *clutter*. In our current exposition, we seek to remove scattering from clutter by modifying the waveforms that are being transmitted into the scene. This is an important task, as scattering from clutter can overpower scattering from targets, rendering the targets difficult to detect or image. *Waveform preconditioning* has been introduced a series of papers by the authors as a way to modify transmit waveforms for better performance in a clutter-rich environment [1–4]. Waveform preconditioning involves determining a filter on the space of transmit waveforms. We refer to this filter as a *preconditioning operator*; it is applied to the transmit waveform prior to transmission. Our primary application is radar imaging. It should be clear, however, that our physics-based approach, where we formulate the problem in terms of Green’s functions and second-order random fields, is applicable to pulse-echo imaging in general, *e.g.*, ultrasound imaging, sonar imaging and microwave imaging.

There are currently two main waveform design approaches in the radar literature: ambiguity-based and variational-based. In the first approach, a range-Doppler echo model is used with matched-filter processing. The waveforms are designed and combined in order to create an approximate Dirac delta ambiguity function [5–13]. In the second approach, the scene is assumed to be static, and therefore, range-only echo models are considered. Similar to the first approach, matched filtering is used as a foundation for joint design of waveforms and receive processing for target detection, identification and classification [14–18]. For target detection, the waveforms are designed by maximizing the signal-to-noise or signal-to-interference ratios [15–17]. A mutual information criteria has also been used to design optimal waveforms for target classification [15].

We derive clutter-rejecting waveforms for pulse-echo measurements from a sparse array of transmitting and receiving elements. The array elements can be distributed spatially in an arbitrary fashion, and can be several hundred wavelengths apart. Such an array is referred to as a *distributed aperture* [19]. Distributed apertures typically view regions of interest that are not in the far-field of the array. This introduces range-dependence in the scattering measurements which cannot be ignored [20, 21]. By using a physics-based measurement model we directly account not only for this range-dependence but also for effects such as multi-path scattering and interference. We incorporate *a priori* statistical information about the scatterers. Furthermore, we allow for multiple transmitters and receivers to be activated simultaneously [22–25], and make no additional assumptions about being able to separate the waveforms from each transmitter by orthogonality [22, 26].

Our analysis leads to explicit expressions for the preconditioning operator involving the Green’s function for the background medium, as well as second-order statistics for the target of interest and the clutter. It turns out, however, that the need for such explicit information can be relaxed by application of the time-reversal principle. The

time-reversal principle is based on an invariance to changing the sign of the temporal variable in the wave equation [27, 28]. It has been used in many applications which involve wave propagation, *e.g.*, ultrasound imaging [28–31], underwater acoustics [32, 33], radar imaging [34, 35], and microwave imaging [36]. Typically, the time-reversal principle is applied successfully to cases where we have a multiple-scattering medium and where explicit modeling of the medium is difficult due to its complexity or due to random perturbations [31, 37–39]. Here, we show how the time-reversal principle can be employed to obtain the preconditioning operator when explicit models for the environment and/or the target and clutter distributions are not available.

From a communications point of view, the radar transmit signal which illuminates the target may be considered as a means for establishing a *communications channel between the target and the observer*. In this language, the effect of a complex environment is considered as part of this communications channel. The goal is to design a filter which, when applied to the transmit signal, shapes the received signal in a desired manner. Thus, there are obvious similarities between the ideas presented here for pulse-echo, and the existing literature on *precoding* [40–42]. However, since our primary aim is to reconstruct the spatial distribution of the target, the spatial aspects of the wave propagation are pronounced in our work.

2. Preliminary notation and modeling

2.1. Distributed aperture

We consider an antenna array consisting of m transmitting elements, and n receiving elements. The placement of these elements can be chosen arbitrarily; the location of each element may be assigned independently of where the other elements are located. For simplicity, we assume each element to behave like an isotropic point antenna; the radiation patterns from each element do not exhibit any directivity. The latter assumption is not needed, but is made in order to keep the analysis more transparent. An important feature of the system under consideration is that we have a reference clock which is common to all of the elements. This common reference clock facilitates *coherent data processing*. An illustration of the distributed nature of an antenna with two transmitting elements and ten receiving elements is shown in Fig. 1.

In order to exploit the spatial diversity inherent in the antenna, it is desirable to allow for transmitting different waveforms from each element. Let $s_j(t)$ denote the waveform which emanates from the j^{th} element. The transmit waveforms are arranged in a *transmit vector* $\mathbf{s}(t)$

$$\mathbf{s}(t) := [s_1(t), \dots, s_m(t)]^T. \quad (1)$$

Similarly, if the measured scattering at the i^{th} receive element is denoted by $m_i(t)$, then the scattering which is collected by the distributed antenna may be arranged in a *measurement vector* $\mathbf{m}(t)$

$$\mathbf{m}(t) := [m_1(t), \dots, m_n(t)]^T. \quad (2)$$

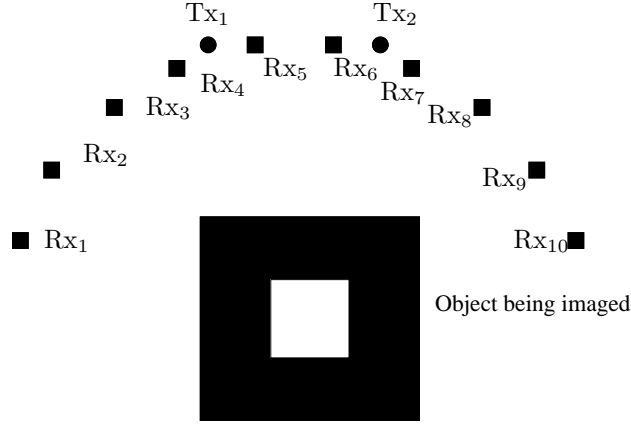


Figure 1. Distributed array with two transmitting elements (circles labeled Tx_1 and Tx_2), and ten receiving elements (small squares labeled from Rx_1 to Rx_{10}). The elements are placed at equidistant points along an arc with radius 10λ , where λ is the wavelength corresponding to the center frequency of the transmitters. The target is indicated as a square with sides of 1.5λ , while the region of interest is $5\lambda \times 5\lambda$ around the target.

2.2. Scattering model

The ability to distinguish scattering objects depends on how much their electromagnetic properties deviate from a known background. We denote this deviation by the reflectivity function $V(\mathbf{x})$. At an abstract level, we denote by $\mathcal{H}(V)$ the operator which maps the transmit vector $\mathbf{s}(t)$ to the measurement vector $\mathbf{m}(t)$

$$\mathbf{m}(t) = \mathcal{H}(V)\mathbf{s}(t). \quad (3)$$

$\mathcal{H}(V)$ is called a scattering operator. An explicit relationship between V and $\mathcal{H}(V)$ can be derived in terms of the *Green's function* $g(\mathbf{x}, \mathbf{y}, t)$ for the background medium. The Green's function is the response measured at position \mathbf{x} from an impulse $\delta(t)$ at position \mathbf{y} . The geometric layout of the antenna elements naturally plays an important role here. Let therefore the j^{th} transmit element be located at position \mathbf{z}_j , and the i^{th} receive element be located at position \mathbf{x}_i . In the current analysis we use a linear scattering model often known as the *distorted-wave Born approximation* [43]. If we define a $(m \times n)$ matrix $G(\mathbf{y}, t)$ with matrix elements

$$G_{ij}(\mathbf{y}, t) := \int g(\mathbf{x}_i, \mathbf{y}, \tau') \partial_t^2 g(\mathbf{y}, \mathbf{z}_j, t - \tau') d\tau', \quad (4)$$

then

$$\mathcal{H}(V)\mathbf{s}(t) := \int G(\mathbf{y}, t - \tau)V(\mathbf{y})d\mathbf{y} \mathbf{s}(\tau)d\tau. \quad (5)$$

Integration in Eq. (5) is understood to be element-wise. For a derivation of Eq. 5, we refer to the Appendix of [44].

2.3. Target and clutter

The above formalism allows us to utilize a physics-based model for the background which in principle can have an arbitrary level of detail. It is not reasonable, however, to expect that our background model will account for all details of the scene except for the target. As outlined in the introduction, this suggests that the reflectivity function should be divided into two parts

$$V(\mathbf{x}) = T(\mathbf{x}) + C(\mathbf{x}). \quad (6)$$

Here $T(\mathbf{x})$ represents *target* and $C(\mathbf{x})$ represents *clutter*. Our definition of clutter includes contributions due to a compromise between model fidelity and tractability: deviations between the background and our model for the background. Our real interest lies in recovering T , while suppressing C .

In our development we assume that $T(\mathbf{x})$ and $C(\mathbf{x})$ are realizations of second-order random fields with known first- and second-order statistics. It should be clear that the background may be defined in such a way that the first-order statistics of the reflectivity functions are zero. Thus, without loss of generality, we will assume that the processes have zero-mean and known auto-correlation functions

$$R_T(\mathbf{y}_1, \mathbf{y}_2) = \mathbb{E} \left[T(\mathbf{y}_1) \overline{T(\mathbf{y}_2)} \right] \quad (7)$$

$$R_C(\mathbf{y}_1, \mathbf{y}_2) = \mathbb{E} \left[C(\mathbf{y}_1) \overline{C(\mathbf{y}_2)} \right]. \quad (8)$$

Furthermore, we will assume that the fields T and C are statistically independent:

$$R_V(\mathbf{y}_1, \mathbf{y}_2) = R_T(\mathbf{y}_1, \mathbf{y}_2) + R_C(\mathbf{y}_1, \mathbf{y}_2). \quad (9)$$

In this work we choose to reject clutter in the minimum-mean-square-error (MMSE) sense: under mild assumptions about the transmit waveforms and the reflectivity functions we can show that $\mathcal{H}(V)$ is a Hilbert-Schmidt (HS) operator [45, Ch. 6.2]. Our goal is therefore to determine a linear operator \mathcal{W} which minimizes $\Delta(W)$

$$\Delta(\mathcal{W}) := \|\mathcal{H}(T + C)\mathcal{W} - \mathcal{H}(T)\|_{\text{HS}}^2. \quad (10)$$

We achieve clutter rejection by employing the transmit waveform $\mathcal{W}s(t)$ instead of $s(t)$. Our approach is illustrated in Fig. 2.

3. The preconditioning operator

In this section we will derive an explicit expression for \mathcal{W} which minimizes the error $\Delta(W)$ as defined in Eq. (10). In order for the analysis to hold, we make certain assumptions about the transmit waveforms and the scattering environment. These assumptions are mild enough to be satisfied for any practical application.

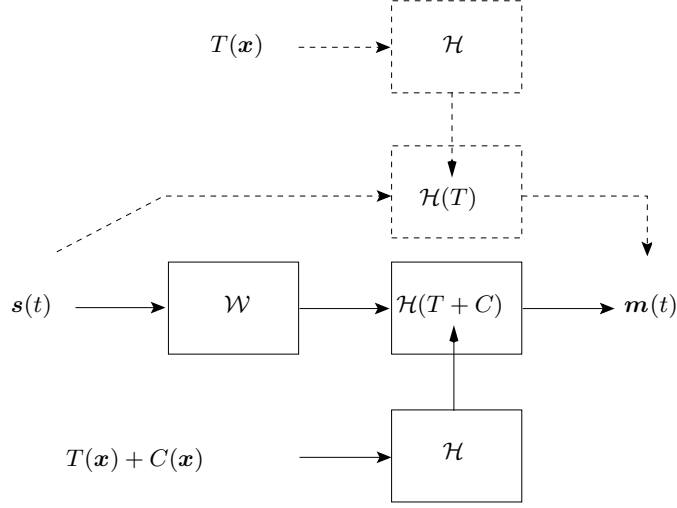


Figure 2. Block diagram for the waveform preconditioning with the operator \mathcal{W} . Solid arrows indicate the signal path from waveform, through preconditioning operator and then transmitted into an environment with system response $\mathcal{H}(T + C)$. Dashed lines indicate the “ideal” signal path which is emulated by applying the preconditioning operator.

First of all, we consider transmit waveforms which have finite length, and which have sufficient decay as a function of frequency. Let the temporal Fourier transform of $s(t)$ be denoted by $\hat{s}(\omega)$. Sufficient decay is guaranteed if we employ the following weighted inner product on the space of transmit waveforms [44]

$$\langle \mathbf{s}_1, \mathbf{s}_2 \rangle = \int (1 + |\omega|^{5+\rho}) \hat{\mathbf{s}}_2^H(\omega) \hat{\mathbf{s}}_1(\omega) d\omega \quad (11)$$

for some $\rho > 0$. Here H denotes conjugate transpose of the vector quantities. Second, it is convenient to assume that no echoes emerge from outside a sufficiently large region, *i.e.*, that the reflectivity function has compact support. Finally, we assume that the environment does not focus the propagating energy onto an arbitrarily small set; no trapped rays exist.

Under the aforementioned assumptions about the waveforms and scattering environment, we can show that $\mathcal{H}(V)$ is a HS operator.

Let $\{e_k(t)\}$ be a basis for the space of transmit vectors. The HS norm of $\mathcal{H}(V)$ can be computed as

$$\|\mathcal{H}(V)\|_{\text{HS}}^2 = \sum_k \int e_k^H(t) \mathcal{H}(V)^* \mathcal{H}(V) e_k(t) dt. \quad (12)$$

Here $*$ denotes the adjoint, and H denotes the conjugate transpose of a vector.

We now determine the operator \mathcal{W} which satisfies Eq. (10). If we require that

$$\Delta(\mathcal{W} + \delta\mathcal{W}) - \Delta(\mathcal{W}) = \mathcal{O}(\|\delta\mathcal{W}\|_{\mathsf{HS}}^2) \quad (13)$$

for all perturbations $\delta\mathcal{W}$, we find that the optimum is

$$\mathcal{W} = [\mathcal{H}(T + C)^* \mathcal{H}(T + C)]^{-1} \mathcal{H}(T)^* \mathcal{H}(T). \quad (14)$$

Define \mathcal{G} as the integral operator with (matrix) kernel $G(\mathbf{y}, t, \tau)$ where the elements of G are given in Eq. 4

$$\mathcal{G}\mathbf{f}(\mathbf{y}, t) := \int G(\mathbf{y}, t - \tau) \mathbf{f}(\tau) d\tau. \quad (15)$$

Define \mathcal{R}_T , and \mathcal{R}_C , as integral operators with (scalar) kernels R_T and R_C from Eqns. 7 and 8, respectively

$$\mathcal{R}_T \mathbf{f}(\mathbf{y}_1) := \int R_T(\mathbf{y}_1, \mathbf{y}_2) \mathbf{f}(\mathbf{y}_2) d\mathbf{y}_2 \quad (16)$$

$$\mathcal{R}_C \mathbf{f}(\mathbf{y}_1) := \int R_C(\mathbf{y}_1, \mathbf{y}_2) \mathbf{f}(\mathbf{y}_2) d\mathbf{y}_2. \quad (17)$$

The operator \mathcal{W} may be expressed as

$$\mathcal{W} = (\mathcal{G}^* [\mathcal{R}_T + \mathcal{R}_C] \mathcal{G})^{-1} \mathcal{G}^* \mathcal{R}_T \mathcal{G}. \quad (18)$$

where \mathcal{G}^* is the adjoint of \mathcal{G} .

The operator \mathcal{W} may be applied to any transmit vector to yield a new transmit vector; \mathcal{W} is a bounded linear operator on the space of transmit vectors.

4. Time-reversal preconditioning

Although Eq. 14 gives an explicit expression for the preconditioning operator, computing the operator is difficult, as it requires a lot of information about the second-order statistics of target and clutter, as well as a model for the background medium. In this section, we will outline an approach which allows us to *estimate* the preconditioning operator from scattering measurements directly.

First, from Eq. (5) we see that $\mathcal{H}(T + C) = \mathcal{H}(T) + \mathcal{H}(C)$. We use this fact to write

$$\mathcal{H}(T) = \mathcal{H}(T + C) - \mathcal{H}(C). \quad (19)$$

Inserting Eq. (19) into Eq.(14) we arrive at

$$\mathcal{W} = I - [\mathcal{H}(T + C)^* \mathcal{H}(T + C)]^{-1} \mathcal{H}(C)^* \mathcal{H}(C) \quad (20)$$

$$= I - [\mathcal{G}^* (\mathcal{R}_T + \mathcal{R}_C) \mathcal{G}]^{-1} \mathcal{G}^* \mathcal{R}_C \mathcal{G}. \quad (21)$$

The last equality follows from Eq. 18. The significant difference between Eq. (14) and (20) is that in Eq. (20) we have replaced $\mathcal{H}(T)^*\mathcal{H}(T)$ by $\mathcal{H}(C)^*\mathcal{H}(C)$. This is important, as $\mathcal{H}(T)$ corresponds to scattering from a target without the presence of clutter, and is infeasible to measure. On the other hand, $\mathcal{H}(C)$ corresponds to scattering from clutter. This can be observed at times when there is no target present.

Consider now the case where there is no target present, and let $c_k(\mathbf{x})$ be a particular clutter realization. By definition, the measured scattering we obtain is $\mathbf{m}_k(t) = \mathcal{H}(c_k)\mathbf{s}(t)$. Furthermore, if we interchange the roles of transmitters and receivers, and transmit $\mathbf{m}_k(-t)$, this corresponds to employing the transpose of the matrix kernel G in Eq. (5), *i.e.*, the measured response at the original transmitters will be

$$\mathbf{q}_k(t) = \int G^T(\mathbf{y}, t - \tau)c_k(\mathbf{y})d\mathbf{y} \mathbf{m}_k(-\tau)d\tau. \quad (22)$$

If we now insert Eqns. 5 into Eq. 22, and express the whole thing in the temporal frequency domain, we get

$$\hat{\mathbf{q}}_k(\omega) = \int \hat{G}^T(\mathbf{y}, \omega)c_k(\mathbf{y})d\mathbf{y} \overline{\hat{\mathbf{m}}(\omega)} \quad (23)$$

$$= \int \hat{G}^T(\mathbf{y}, \omega)c_k(\mathbf{y})d\mathbf{y} \overline{\int \hat{G}(\mathbf{x}, \omega)c_k(\mathbf{x})d\mathbf{x}\hat{\mathbf{s}}(\omega)} \quad (24)$$

$$= \int \hat{G}^H(\mathbf{y}, \omega)\overline{c_k(\mathbf{y})}c_k(\mathbf{x})\hat{G}(\mathbf{x}, \omega)d\mathbf{x}d\mathbf{y}\hat{\mathbf{s}}(\omega). \quad (25)$$

Let us now average this experiment over multiple realizations of the clutter to form

$$\mathbf{p}(t) := \frac{1}{N} \sum_{k=1}^N \mathbf{q}_k(-t). \quad (26)$$

Then

$$\mathbf{p}(t) = \frac{1}{N} \sum_{k=1}^N \int \hat{G}^H(\mathbf{y}, \omega)\overline{c_k(\mathbf{y})}c_k(\mathbf{x})\hat{G}(\mathbf{x}, \omega)d\mathbf{x}d\mathbf{y}\hat{\mathbf{s}}(\omega) \quad (27)$$

$$\approx \int \hat{G}^H(\mathbf{y}, \omega)\mathbb{E}[\overline{c_k(\mathbf{y})}c_k(\mathbf{x})]\hat{G}(\mathbf{x}, \omega)d\mathbf{x}d\mathbf{y}\hat{\mathbf{s}}(\omega) \quad (28)$$

$$= \int \hat{G}^H(\mathbf{y}, \omega)R_C(\mathbf{x}, \mathbf{y})\hat{G}(\mathbf{x}, \omega)d\mathbf{x}d\mathbf{y}\hat{\mathbf{s}}(\omega). \quad (29)$$

This is a frequency-domain expression for $\mathcal{G}^*\mathcal{R}_C\mathcal{G}\mathbf{s}(t)$. Therefore, $\mathbf{p}(t)$ will be an approximation for $\mathcal{G}^*\mathcal{R}_C\mathcal{G}\mathbf{s}(t)$.

Under the assumption that there is no target present in the scene, the following algorithm will allow us to obtain $\mathcal{G}^* \mathcal{R}_C \mathcal{G}$ applied to a transmit vector \mathbf{s} :

1. Transmit waveform $\mathbf{s}(t)$ and obtain measurement $\mathbf{m}_k(t)$.
2. Interchange the role of transmitters and receivers
3. Transmit waveform $\mathbf{m}_k(-t)$ and obtain measurement $\mathbf{q}_k(t)$.
4. Repeat multiple times to obtain the estimate

$$\mathbf{p}(t) = \frac{1}{N} \sum_{k=1}^N \mathbf{q}_k(-t) \approx \mathcal{G}^* \mathcal{R}_C \mathcal{G} \mathbf{s}(t) \mathbf{s}(t)$$

The same procedure will allow us to determine $\mathcal{H}(T+C)^* \mathcal{H}(s(t))$ from data containing scattering from both target and clutter. We can thus estimate the required information for computing \mathcal{W} as defined in Eq. 21.

We can also get to $\mathcal{H}(C)^* \mathcal{H}(C) \mathbf{s}(t)$ by applying a zero-phase filter with frequency response $1/(1 + |\omega|^{5+\rho})$. The advantage of seeking $\mathcal{H}(C)^* \mathcal{H}(C) \mathbf{s}(t)$ is that repeated iteration will allow us to obtain eigenvalues and eigenfunctions of this operator (we have a self-adjoint, compact operator on the space of transmit waveforms).

5. Numerical simulation

In order to demonstrate the clutter-suppression obtained with our waveform preconditioning operator, we have performed a set of numerical simulations. In these simulations we want to recover the target T from scattering measurements made with two transmitters and ten receivers. The transmitters and receivers were placed equally spaced on an arc around the target. This simulation setup is illustrated in Fig. 1.

From the two transmitters we transmitted short chirp signals: Transmitter 1 emitted a linear up-chirp, while Transmitter 2 emitted a linear down-chirp. All dimensions of the experiment were normalized according to a unit length scale λ .

As a target we chose a square with sides $1.5\lambda \times 1.5\lambda$. From this target model we constructed a target spectrum as if the target were a realization of a stationary random field. A high-frequency version of the stationary stochastic target model was then constructed and used to simulate different realizations of the surrounding clutter. This construction is explained further in Yazıcı *et al.* [46]. The compact support of the clutter was imposed by applying a spatial mask. For our purpose we used a region of $5\lambda \times 5\lambda$ around the target. Finally, the radius of the arc on which the antenna elements were placed was set to 10λ .

The preconditioning operator was constructed according to Eq. (14) from 50 estimated eigenvalues and eigenvectors for $\mathcal{H}(C)^* \mathcal{H}(C)$ and $\mathcal{H}(T+C)^* \mathcal{H}(T+C)$ by a Monte-Carlo approach. The spatial discretization for each scattering simulation was 15 samples per wavelength λ .

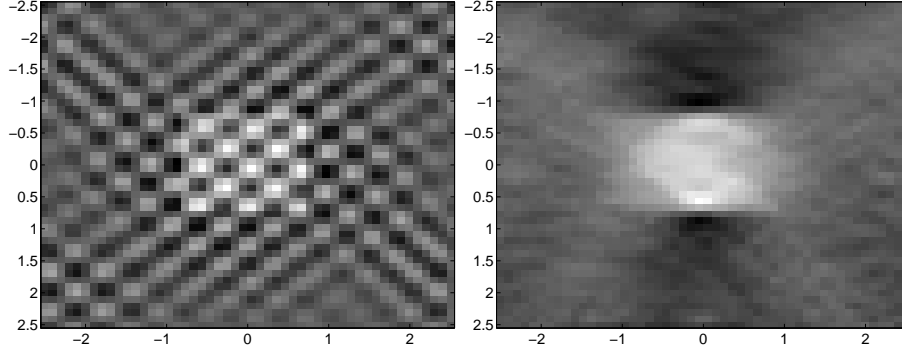


Figure 3. Target with clutter (left) and reconstruction of target from clutter-free scattering (right)

The signal-to-clutter ratio (SCR) in our simulations was set to -6 dB, when defined according to

$$\text{SCR} = 10 \log \left(\frac{\int \mathbb{E}[|T(\mathbf{x})|^2] d\mathbf{x}}{\int \mathbb{E}[|C(\mathbf{x})|^2] d\mathbf{x}} \right). \quad (30)$$

The performance of the preconditioning was evaluated by observing the square error in the reconstructed image when compared to the true reflectivity function. The mean-square-error (MSE) was estimated by averaging over 10 clutter realizations. We computed the MSE according to

$$\text{MSE}(\mathcal{W}) = 10 \log \left(\frac{\int \mathbb{E}[|\mathcal{H}^{-1}\mathcal{H}(T + C)\mathcal{W}(\mathbf{x}) - T(\mathbf{x})|^2] d\mathbf{x}}{\int \mathbb{E}[|T(\mathbf{x})|^2] d\mathbf{x}} \right). \quad (31)$$

We employed the imaging method proposed in [44] to form the images. This method is well suited to work with waveform preconditioning, as it is capable of handling scattering from multiple sources simultaneously, and is based on the same figure of merit as our current preconditioning work; it forms the optimal image in a MSE sense. The images were reconstructed on a grid with 10 samples per wavelength.

Figure 3 shows the target embedded in clutter, as well as a reconstructed image based on scattering without clutter. The MSE in this case was 3.5 dB.

Figure 4 show reconstruction results for scattering with clutter. Preconditioning of the transmit waveform improves image quality from 8.9 dB to 4.3 dB when measured using the MSE defined in Eq. (31).

Figure 5 shows the spectrum of one of the transmit waveform that were employed in this experiment.

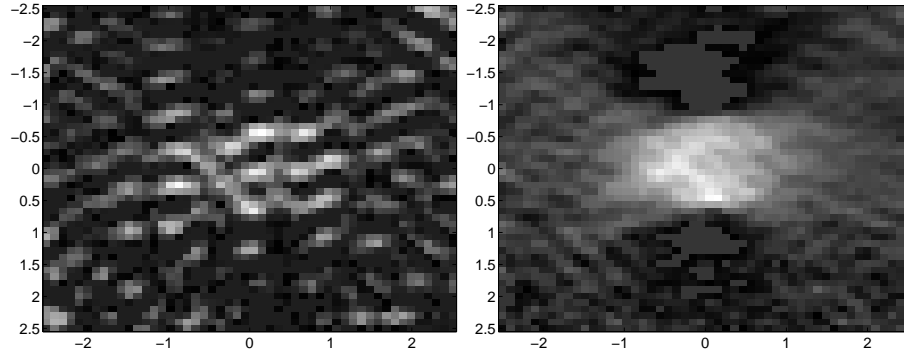


Figure 4. Reconstruction results for a single realization of clutter. Left: image from scattering with original chirp waveform. Right: image from scattering with preconditioned chirp waveform

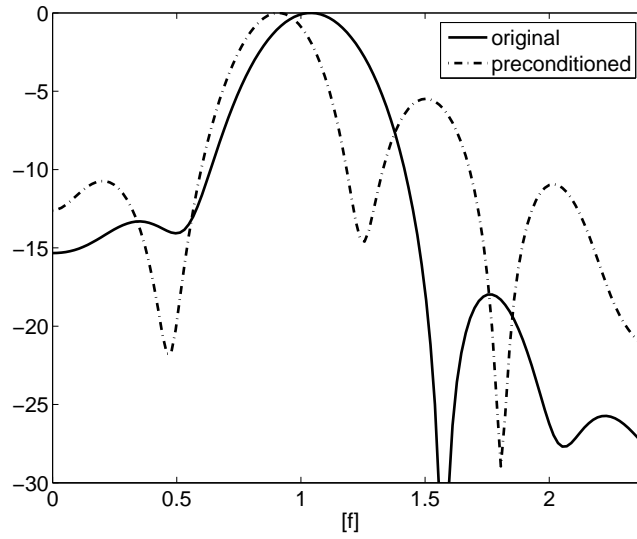


Figure 5. Spectrum magnitude (right) for the original waveform, and for the preconditioned waveform.

6. Discussion and concluding remarks

In this work we have separated the reflectivity function into two distinct classes: *target* and *clutter*. The clutter essentially produces unwanted scattering which in turn degrades the final result of the reconstructed image. If scattering from clutter can be removed from the measurement, the end result will be improved. Our preconditioning operator can be applied to any set of transmit vectors in order to optimally reject scattering from clutter in the MMSE sense.

Our analysis is based on assumed *a priori* knowledge about the scene in the form of the Green's function, and about the target and clutter distribution in the form of first and second-order statistics. We used the Green's function to map second-order statistics of the clutter and target to the space of transmit vectors and thereby construct the preconditioning operator. Finally, we point out how the time-reversal principle can be applied to alleviate the need for explicit knowledge about the Green's function and the target/clutter distributions.

We address the problem of optimally modifying the transmit waveform when the transmit power is limited. Obviously, after preconditioning the resulting waveform may not have the same strength. However, this is trivially amended by proper normalization of the preconditioned waveform. As a result, the transmit vector will contain the same amount of power, but will minimize scattering from clutter. Hence, for a fixed total transmit power, the SCR may be improved in the final image. Alternatively, for a given signal-to-noise ratio in the final image the total transmit power can be reduced. This is of interest in applications where it is desirable to keep the transmit power as low as possible, *e.g.*, to reduce transmitter vulnerability/detectability.

When we perform clutter rejection we identify a transmit-vector subspace where the signal-to-clutter (SCR) ratio is high. The fact that the signals which are employed at each transmitter are transmitted simultaneously, and that they are not orthogonal imply that there is a great deal of ambiguity in the data with respect to the correct time-of-flight for a given echo. We therefore have limited ability to determine the correct source-receiver pair for a given echo. As we are forming the images using a our limited-angle tomographic approach, we do not rely on the ability to resolve the source-receiver ambiguity [44].

The underlying propagation model which we have used for this work is derived from a scalar wave equation. This is a commonly-used model for many radar applications where polarization effects may be ignored. In order to get explicit expressions in terms of Green's functions, a linearized scattering model was used, namely the distorted-wave Born approximation (DWB). Note, however, that the operator norm which we used to determine the preconditioning operator will make sense also without the DWB. The time-reversal principle also holds in other pulse-echo applications. Our work therefore has applications also in other areas such as ultrasound, sonar and microwave imaging.

ACKNOWLEDGMENTS

We are grateful to Air Force Office of Scientific Research¹ (AFOSR) and the Defense Advanced Research Projects Agency (DARPA) for supporting this work under the agreements FA9550-04-1-0223, FA9550-06-1-0017 and FA8750-05-2-0285.

References

- [1] B Yazıcı and G Xie, “Wideband extended range-Doppler imaging and waveform design in the presence of clutter and noise,” *IEEE Trans. Inf. Theory*, vol. 52, no. 10, 2006.
- [2] T Varslot, B Yazıcı, C E Yarman, M Cheney, and L Sharf, “Waveform preconditioning for clutter rejection,” in *Proc. 2007 SPIE Defense and Security Conference*, 2007, p. 6568N.
- [3] T Varslot, B Yazıcı, C E Yarman, M Cheney, and L Sharf, “Time-reversal waveform preconditioning for clutter rejection,” in *Proc. 3rd International IEEE Conference in Waveform Design and Diversity*, 2007, p. 4016.
- [4] T Varslot, B Yazıcı, C E Yarman, M Cheney, and L Sharf, “Waveform preconditioning for clutter rejection in multipath for sparse distributed apertures,” in *Proc. of The Second International Workshop on Computational Advances in Multi-Sensor Adaptive Processing (COMSAP)*, December 2007.
- [5] R. H. Barker, *Group synchronizing of binary digital systems*, pp. 273–287, Academic Press, New York, 1953.
- [6] R. L. Frank, “Polyphase codes with good nonperiodic correlation properties,” *IEEE Trans. Inf. Theory*, vol. 9, no. 1, pp. 43–45, 1963.
- [7] R. Sivaswamy, “Digital and analog subcomplementary sequences for pulse compression,” *IEEE Trans. Aerosp. Electron. Syst.*, vol. AES-14, pp. 343–350, 1978.
- [8] R Sivaswamy, “Multiphase complementary codes,” *IEEE Trans. Inf. Theory*, vol. IT-24, no. 5, pp. 546–552, 1978.
- [9] J. P. Costas, “A study of a class of detection waveforms having nearly ideal range-doppler ambiguity properties,” *Proc. IEEE*, vol. 72, no. 8, pp. 996–1009, 1984.
- [10] S. W. Golomb and H. Taylor, “Constructions and properties of costas arrays,” *Proc. IEEE*, vol. 72, no. 9, pp. 1143–1163, 1984.

¹Consequently, the US Government is authorized to reproduce and distribute reprints for governmental purposes notwithstanding any copyright notation thereon. The views and conclusions contained herein are those of the authors and should not be interpreted as necessarily representing the official policies or endorsements, either expressed or implied, of the Air Force Research Laboratory or the US Government.

- [11] S. W. Golomb and H. Taylor, "Algebraic construction of costas arrays," *J. Comb. Theory, ser. A*, vol. 37, pp. 13–21, 1984.
- [12] J.C. Guey and M.R. Bell, "Diversity waveform sets for delay-doppler imaging," *IEEE Transactions on Information Theory*, vol. 44, no. 4, pp. 1504 – 1522, 1998.
- [13] C. Chang and M. R. Bell, "Frequency-coded waveforms for enhanced delay-doppler resolution," *IEEE Trans. Inf. Theory*, vol. 49, no. 11, pp. 2960–2971, 2003.
- [14] D. T. Gjessing, *Target Adaptive Matched Illumination Radar: Principles and Applications*, Peter Peregrinus, Stevenage, U.K., 1986.
- [15] M Bell, "Information theory and radar waveform design," *IEEE Trans. Inf. Theory*, vol. 39, no. 5, pp. 1578–1597, September 1993.
- [16] S U Pillai, H S Oh, D C Youla, and J R Guerci, "Optimum transmit-receiver design in the presence of signal-dependent noise and channel noise," *IEEE Trans. Inf. Theory*, vol. 46, no. 2, pp. 577–584, 2000.
- [17] D. A. Garren, M. K. Osborn, A. C. Odom, J. S. Goldstein, S. U. Pillai, and J. R. Guerci, "Enhanced target detection and identification via optimized radar transmission pulse shape," *Proc. IEE, Radar, Sonar and Navigation*, vol. 148, no. 3, pp. 130–138, 2001.
- [18] S.M. Sowelam and A. H. Tewfik, "Waveform selection in radar target classification," *IEEE Transactions on Information Theory*, vol. 46, no. 3, pp. 1014–1029, 2000.
- [19] R Adve, R Schneibler, G Genello, and P Antonik, "Waveform-space-time adaptive processing for distributed aperture radars," in *Proc. 2005 IEEE Radar Conf.*, 2005, pp. 93–97.
- [20] R Adve, R Schneibler, and R McMillan, "Adaptive space/frequency processing for distributed apertures," in *Proc. 2003 IEEE Radar Conf.*, 2003, pp. 160–164.
- [21] R Adve, "Sub-optimal adaptive processing for distributed aperture radars," in *Proc. 2nd Waveform Diversity Workshop*, Verona, NY, 2003, pp. 160–164.
- [22] E Fishler, A Haimovich, R Blum, L Cimini, D Chizhik, and R Valenzuela, "Spatial diversity in radars - models and detection performance," *IEEE Trans. Sign. Processing*, vol. 54, no. 3, pp. 823–238, 2006.
- [23] I Bekkerman and J Tabrikian, "Target detection and localization using MIMO radars and sonars," *IEEE Tran. Signal Proc.*, vol. 54, no. 10, pp. 3873–3883, 2006.
- [24] A Fletcher and F Robey, "Performance bounds for adaptive coherence of sparse array radar," in *Proc. of 11th. Conf. Adaptive Sensors Array Processing, Lexington (MA)*, March 2003.

- [25] D Rabideau, "Ubiquitous mimo digital array radar," in *Proc. 37th Asilomar Conf. Signals, Systems, Computers*, 2003.
- [26] E Bond, S Hagness, and B Veen, "Microwave imaging via space-time beam-forming for early detection of breast cancer," *IEEE Trans. Ant. Prop.*, vol. 51, no. 8, pp. 1690–1705, 2003.
- [27] M Fink, "Time-reversed acoustics," *Scientific American*, vol. 281, pp. 91–97, Nov 1999.
- [28] M Fink, "Time reversal of ultrasonic fields - part I: Basic principles," *IEEE Trans. Ultrason. Ferroelectr. Freq. Control*, vol. 39, pp. 555–567, 1992.
- [29] C Prada, J L Thomas, and M Fink, "The iterative time reversal process: analysis of convergence," *J. Acoust. Soc. Am.*, vol. 97, no. 1, pp. 62–71, January 1995.
- [30] M Tanter, J-L Thomas, and M Fink, "Time reversal and the inverse filter," *J. Acoust. Soc. Am.*, vol. 108, no. 1, pp. 223–234, July 2000.
- [31] G Montaldo, D Palacio, M Tanter, and M Fink, "Building three-dimensional images using a time-reversal chaotic cavity," *IEEE Trans. Ultrason. Ferroelectr. Freq. Control*, vol. 52, no. 9, pp. 1489–1497, September 2005.
- [32] G F Delmann, H C Song, S Kim, W S Hodgkiss, W A Kuperman, and T Akal, "Underwater acoustic communications using time reversal," *IEEE J Oceanic Engineering*, vol. 30, no. 4, pp. 852–864, 2005.
- [33] H C Song, W S Hodgkiss, W A Kuperman, M Stevenson, and T Akal, "Improvement of time-reversal communications using adaptive channel equalizers," *IEEE J Oceanic Eng.*, vol. 31, no. 2, pp. 487–496, 2006.
- [34] D Liu, G Li, Y Chen, S Vasudevan, W Jones, Q Liu, J Krollik, and L Carin, "Electromagnetic time-reversal imaging of a target in a cluttered environment," *IEEE Trans. Ant. Prop.*, vol. 53, no. 9, pp. 3058–3066, 2005.
- [35] A Devaney, "Time reversal imaging of obscured targets from multistatic data," *IEEE Trans. Ant. Prop.*, vol. 53, no. 5, pp. 1600–1610, 2005.
- [36] P Kosmas and C M Rappaport, "A matched-filter fdtd-based time reversal approach for microwave breast cancer detection," *IEEE Trans. Ant. and Prop.*, vol. 54, no. 4, pp. 1257–1264, 2006.
- [37] P Blomgren, G Papanicolaou, and H Zhao, "Super-resolution in time-reversal acoustics," *J. Acoust. Soc. Am.*, vol. 111, no. 1, pp. 203–248, 2002.
- [38] C Oestges, A D Kim, G Papanicolaou, and A.J. Paulraj, "Characterization of space-time focusing in time reversed random fields," *IEEE Trans. Ant. and Prop.*, vol. 53, no. 1, pp. 283–293, 2005.

- [39] G Papanicolaou, L Ryzhik, and K Solna, “Statistical stability in time reversal,” *SIAM J. Appl. Math.*, vol. 64, pp. 1133–1155, 2004.
- [40] G Forney and M Eyuboglu, “Combined equalization and coding using precoding,” *IEEE Comm Mag*, Dec 1991.
- [41] H Harashima and H Miyakawa, “Matched transmission technique for channels with intersymbol interference,” *IEEE Trans. Commun.*, vol. COM-20, pp. 774–780, 1972.
- [42] M Tomlinson, “New automatic equalizer employing modulo arithmetic,” *Electron. Lett.*, vol. 7, pp. 138–139, 1971.
- [43] J H Taylor, *Scattering Theory*, Wiley, New York, 1972.
- [44] T Varslot, B Yazıcı, and M Cheney, “Wide-band pulse-echo imaging with distributed apertures in multi-path environments,” *Inverse Problems*, vol. 24, pp. 1–28, 2008.
- [45] J Weidmann, *Linear Operators in Hilbert Spaces*, Springer-Verlag, New York, 1980.
- [46] B Yazıcı, M Cheney, and C E Yarman, “Synthetic aperture inversion for an arbitrary flight trajectory in the presence of noise and clutter,” *Inverse Problems*, vol. 22, no. 5, pp. 1705–1729, 2006.